RSC Advances

PAPER

View Article Online
View Journal | View Issue

Cite this: *RSC Adv.*, 2021, **11**, 8879

Step-saving synthesis of star-shaped hole-transporting materials with carbazole or phenothiazine cores *via* optimized C–H/C–Br coupling reactions†

Jui-Heng Chen,[a] Kun-Mu Lee,*[b] Chang-Chieh Ting[a] and Ching-Yuan Liu *[a]

Received 3rd December 2020
Accepted 15th February 2021

DOI: 10.1039/d0ra10190g

rsc.li/rsc-advances

In most research papers, synthesis of organic hole-transporting materials relies on a key-reaction: Stille cross-couplings. This requires tedious prefunctionalizations including the preparation and treatment of unstable organolithium and toxicity-concern organotin reagents. In contrast to traditional multistep synthesis, this work describes that a series of star-shaped small molecules with a carbazole or phenothiazine core can be efficiently synthesized through a shortcut using optimized direct C–H/C–Br cross-couplings as the key step, thus avoiding dealing with the highly reactive organolithium or the toxic organotin species. Device fabrication of perovskite solar cells employing these molecules (**6–13**) as hole-transporting layers exhibit promising power conversion efficiencies of up to 17.57%.

Introduction

Perovskite solar cells (PSCs) using organic molecules as hole-transporting materials (HTMs) have attracted significant research interest because of their promising power conversion efficiencies (PCE).[1–13] Compared to π-conjugated polymers, oligomers possess several advantages including well-defined conjugation lengths, flexible molecular design and reproducible chemical synthesis with higher compound purities.[14–21] By far, 2,2′,7,7′-tetrakis(*N*,*N*-di-*p*-methoxyphenylamino)-9,9′-spirobifluorene (**spiro-OMeTAD**) is the most used organic HTM in perovskite-based solar cells.[22] However, it was also stated that **spiro-OMeTAD** owns a number of drawbacks such as low conductivity, low hole-mobility, and high commercial price. Besides, synthetically speaking, accessing **spiro-OMeTAD** requires costly spirobifluorene as starting material. Therefore, present research attention has been switched to the development of non-spirolinked small molecules.[23] Among various nonspiro-type building blocks, triphenylamine (TPA), carbazole (Cbz), and phenothiazine (PTZ) were very attractive to material scientists since they are inexpensive, readily available and usually exhibit remarkable PCEs while incorporated in PSCs as hole-transport layers.[24] Recently, we also demonstrated a series of small-molecule HTMs incorporating TPA- or Cbz-derivatives as end-groups for efficient PSCs.[25] However, we have noticed that the employment of Cbz or PTZ as core-moiety still remained less explored. Even though few examples were reported, synthetic approaches for these HTMs were neither step-economical nor optimized.[24,26] Moreover, we envisaged that introduction of a carbazole or phenothiazine group as core for HTMs might further improve their hole-mobilities and the performance of PSCs. Therefore, we report herein, an efficient access to eight star-shaped new molecules with Cbz- or PTZ-

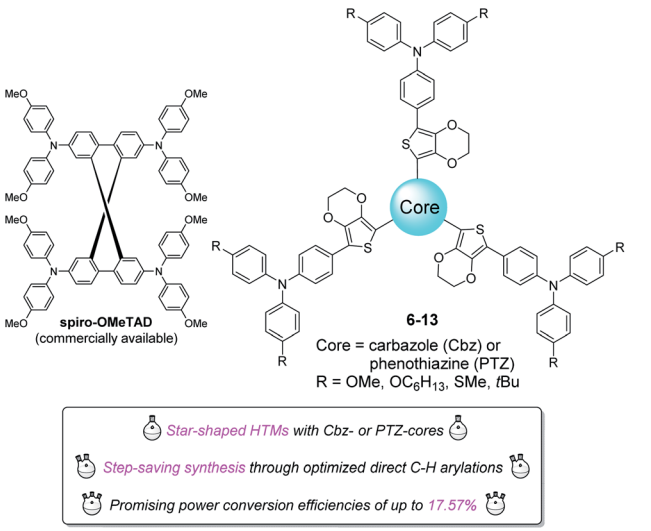

Fig. 1 Eight star-shaped HTMs with carbazole or phenothiazine cores: step-saving synthesis and application for perovskite solar cells.

[a]*Department of Chemical and Materials Engineering, National Central University, Jhongli District, Taoyuan 320, Taiwan, Republic of China. E-mail: cyliu0312@ncu.edu.tw*

[b]*Department of Chemical and Materials Engineering, Chang Gung University, Department of Pediatrics, Chang Gung Memorial Hospital, Linkou, Taoyuan 333, Taiwan, Republic of China. E-mail: kmlee@mail.cgu.edu.tw*

† Electronic Supplementary Information (ESI) available: NMR spectra (^{1}H and ^{13}C) of compounds **6–13**. See DOI: 10.1039/d0ra10190g

cores (Cbz: carbazole for **6–9**; PTZ: phenothiazine for **10–13**) through a step-saving synthetic strategy under pre-optimized direct C–H arylation reaction conditions (Fig. 1). Property and photovoltaic performance of perovskite solar cells using these compounds as HTMs were also investigated.

Results and discussion

In Scheme 1, a comparison of two synthetic pathways to **JHC01–08** was demonstrated. Traditionally, as shown in pathway A, the end-group molecules **3a–d** [11] underwent deprotonation with *n*-butyl lithium at low temperature (usually −78 °C) to give unstable organolithium intermediates **4** which were subsequently transmetalated with trialkyltin chloride to afford organotin reagents **5**. The final products can be readily reached by performing Stille cross-coupling reactions of **5** with the core molecules (**1** or **2**), even though the preparation and treatment of organotin species is toxicity-concerned and time-consuming. On the other hand, in pathway B, we proposed a step-saving shortcut to **6–13** *via* direct C–H bond activation/arylation of **3a–d** with core **1** or **2**, by which the generation of organolithium and the contact of organotin compounds can be entirely avoided.

Based on pathway B, we carried out a facile synthesis of **6–13**. In order to find optimum reaction conditions, the direct C–H/C–Br cross-coupling was investigated using core **1** and end **3a** as model study focusing on ligand screening. First, as shown in Table 1, reaction of **3a** with tribromocarbazole was conducted under general C–H activation/arylation conditions: $Pd(OAc)_2$, PPh_3, PivOH, and K_2CO_3 in DMF (125 °C, 30 h), giving desired **6** in 38% (isolated yield, entry 1). Other triarylphosphine monodentate ligands were also examined to produce **6** in 29–57% yields (entries 2–4). *N*-Heterocyclic carbene (NHC) ligand such as IPr gave product in 38% (entry 5). The C–H arylation was then performed with three phosphine ligands bearing alkyl groups (entries 6–8), furnishing **6**

Table 1 Ligand screening for the optimization of direct C–H arylations using core **1** and end **3a**[a]

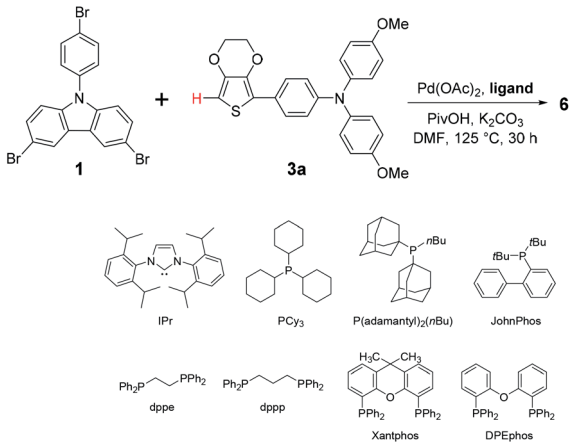

Entry	Ligand	Yield[b] (%)
1	PPh_3	38
2	P(*o*-tolyl)$_3$	57
3	P(*m*-tolyl)$_3$	29
4	Tris(*o*-methoxyphenyl)phosphine	53
5	IPr	38
6	P(Cy)$_3$	51
7	P(adamantyl)$_2$(*n*Bu)	62
8	JohnPhos	35
9	dppe	20
10	dppp	23
11	Xantphos	21
12	DPEphos	18
13[c]	P(*o*-tolyl)$_3$	70
14[c]	P(adamantyl)$_2$(*n*Bu)	67

[a] Direct C–H arylation of **3a** (0.96 mmol) with **1** (0.30 mmol) was conducted under N_2 in the presence of $Pd(OAc)_2$ (15 mol%), ligand (30 mol%), pivalic acid (60 mol%), and K_2CO_3 (1.08 mmol) in DMF (3 mL) at 125 °C for 30 h. [b] Isolated yields. [c] 1 mL DMF was used.

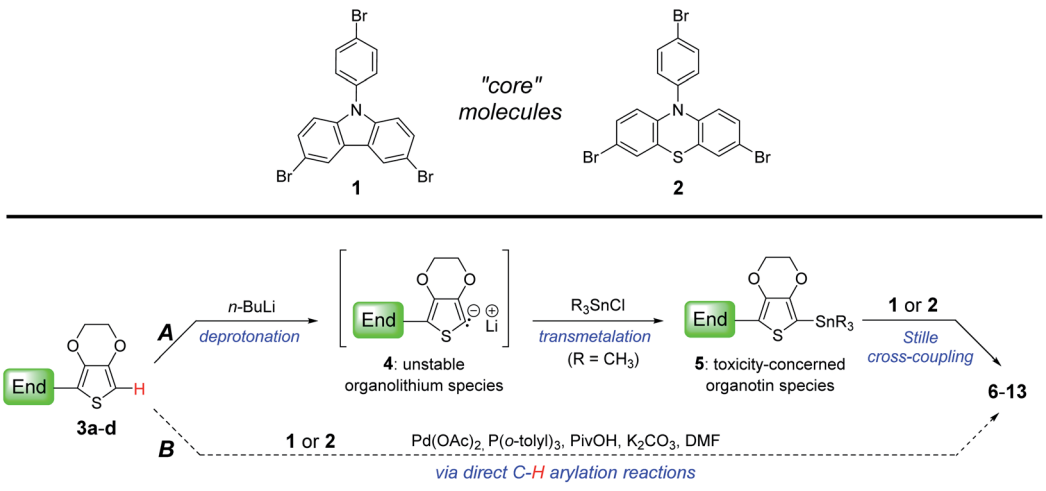

***Pathway A**: traditional multi-step synthesis vs. **Pathway B**: step-saving synthesis shortcut (This Work)*

Scheme 1 Comparison of two synthetic pathways: multi-step *versus* step-saving synthesis of **6–13**.

of up to 62% isolated yield. From entry 9 to 12, the bidentate phosphine ligands had also been tested. However, they were shown to be less efficient toward C–H/C–Br coupling reactions, providing **6** in only 18–23% yields.

According to above results, we selected P(*o*-tolyl)$_3$ (entry 2) and P(adamantyl)$_2$(*n*Bu) (entry 7) as the optimum ligands for additional examinations. In last two entries (13 and 14), the direct C–H arylations proceeded under a more concentrated condition (solvent reduced to 1 mL) and we were pleased to find the yield of **6** could be further improved (67–70%).

Therefore, in Scheme 2, we decided to use P(*o*-tolyl)$_3$ for the efficient synthesis of other HTM molecules (**7–9** with a Cbz core; **10–13** with a PTZ core) because of its lower commercial price. In addition to the methoxy group (–OMe) that was often equipped with small-molecule HTMs, we also explored other potential and previously used end-substituents[11] including *n*-hexyloxy group (–OC_6H_{13}), methyl sulfide group (–SMe) and tertiary-butyl group (–*t*Bu). Reaction of **3b** (R = OC_6H_{13}) with either core-**1** (Cbz) or -**2** (PTZ) under optimum reaction conditions produced **7** or **11** in moderate isolated yields (62%; 65%). These two compounds exhibited fairly good solubility in common organic solvents owing to their longer alkyl chains, which might be beneficial to follow-up solution-based device fabrication and film formation through spin-coating techniques.

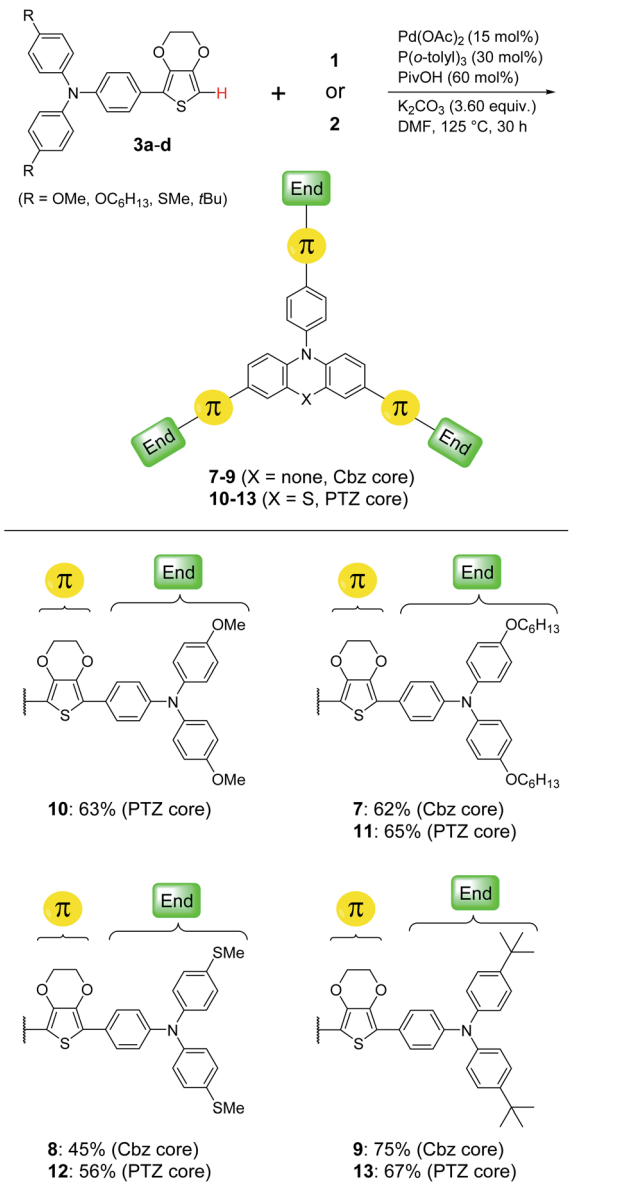

Scheme 2 Synthesis of **7–13** under optimum reaction conditions.

Next, we investigated the optical, electrochemical, electrical and thermal properties of synthesized **6–13** and the results were summarized in Table 2 (relevant spectra were provided in ESI†). In general, the PTZ core-based **10–13** possess smaller optical bandgaps (ΔE_g = 2.56–2.57 eV) than Cbz core-based **6–9** (ΔE_g = 2.73–2.81 eV). Based on the electrochemical measurements and calculations, we obtained each E_{HOMO} (the highest occupied molecular orbital) of eight HTM molecules, all of which were located between the E_{HOMO} of perovskite layer ($MAPbI_3$, E_{HOMO} = −5.43 eV) and Ag electrode (E_{HOMO} = −4.20 eV), revealing that **6–13** had appropriate energy levels to serve as potential hole-transport materials. In addition, the hole-mobility (μ_h) of **6–13** was evaluated by measuring their current density–voltage ($J - V$) in the region of space-charge limited current (SCLC). It was found that, HTMs bearing –*t*Bu groups (**9** and **13**) exhibited outstanding hole mobilities (μ_h = 6.46 × 10^{-4} and 7.53 × 10^{-4} cm^2 V^{-1} s^{-1}) that are close to the μ_h of **spiro-OMeTAD** (8.38 × 10^{-4} cm^2 V^{-1} s^{-1}). Among all HTMs, the molecules with –SMe groups (**8** and **12**) showed the lowest hole mobilities (μ_h = 1.35 × 10^{-4} and 6.68 × 10^{-5} cm^2 V^{-1} s^{-1}), which implied that –SMe might not be a suitable substituent for the design of small-molecule HTMs. We also obtained the thermal analysis data of all HTMs. It is interesting to note that, except for hole mobilities, **9** and **13** (with *t*Bu groups) also showed superior decomposition temperature (T_d = 426 °C; 415 °C) and glass transition temperature (T_g = 223 °C; 228 °C) than those of other HTM molecules. Among eight

Table 2 Summary of the optical, electrochemical, electrical and thermal properties of **6–13**

HTMs	ΔE_g[a] [eV]	E_{HOMO}[b] [eV]	E_{LUMO}[c] [eV]	Hole mobility (cm^2 V^{-1} s^{-1})	T_d [°C]	T_g [°C]
6	2.76	−5.21	−2.45	1.71 × 10^{-4}	370	177
7	2.73	−5.20	−2.47	1.59 × 10^{-4}	396	88
8	2.81	−5.25	−2.46	1.35 × 10^{-4}	406	192
9	2.78	−5.21	−2.43	6.46 × 10^{-4}	426	223
10	2.57	−5.16	−2.59	2.34 × 10^{-4}	406	184
11	2.56	−5.20	−2.64	4.10 × 10^{-4}	382	91
12	2.57	−5.22	−2.65	6.68 × 10^{-5}	387	192
13	2.56	−5.20	−2.64	7.53 × 10^{-4}	415	228

[a] ΔE_g was calculated based on the spectra of UV/vis absorption and photoluminescence (measurements performed in CH_2Cl_2). [b] E_{HOMO} = −[$E_{1/2}$ (*vs.* $Ag/AgCl_{sat'd}$) + 0.197 (*vs.* NHE) + 4.500] eV (the electrochemical experiments were performed in CH_2Cl_2). [c] E_{LUMO} = E_{HOMO} + ΔE_g.

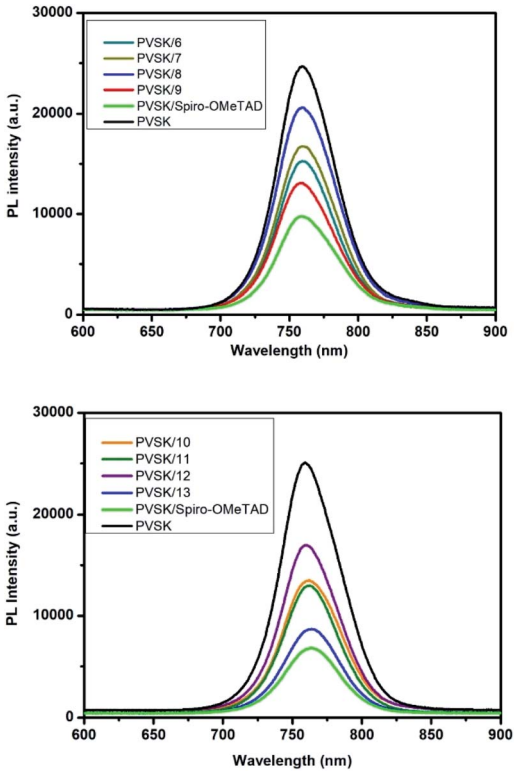

Fig. 2 The steady-state photoluminescence spectra of devices fabricated as: glass/$MAPbI_3$ (perovskite layer)/**6–13** (hole-transport layer).

HTMs, **7** and **11** carrying long alkoxyl groups ($-OC_6H_{13}$) demonstrated obviously lower T_g (88–91 °C), presumably resulting from the thermally caused motion of alkyl chains.[27,28] Furthermore, we studied the hole-extraction capability of eight molecules by conducting the experiments of steady-state photoluminescence (PL). The required devices were fabricated as glass/$MAPbI_3$/**6–13**, respectively. The spectra provided in Fig. 2 revealed that **9** & **13** (*t*Bu groups) had remarkable PL quenching abilities. This implied they could extract holes efficiently from the interface between perovskite- and hole-transport layers, whereas the **8** & **12** (–SMe groups) showed poor hole-extraction capabilities.[29] We speculated this might be attributed to the inferior coordination of methyl sulfide groups to the perovskite layer.

Device fabrication of perovskite solar cells using **6–13** as hole-transporting layers was detailed in ESI.† In general, **6–13** was each dissolved in chlorobenzene and the solutions were heated to 90–100 °C to ensure the HTM molecule was completely dissolved. Each solution was then doped with lithium bis(trifluoromethane)sulfonimide (Li-TFSI) and 4-*tert*-butylpyridine (TBP). After the PSC devices were obtained *via* spin-coating techniques, we evaluated their photovoltaic performances and the data were summarized in Table 3. It is interesting to note that PSCs based on **9** and **13** (with *t*Bu groups) showed exceptional power conversion efficiencies (PCEs = 17.51%, 17.57%) regardless of the variation of their core molecules (Cbz or PTZ), which is comparable to the PCE of reference cells (**spiro-OMeTAD**, PCE = 17.65%). Based on the high T_g of **9** and **13** shown in last section (Table 2), we speculated that PSC devices incorporating **9**- or **13** as hole-transporting layer might possess more stable film morphology at high operational temperature, thus leading to higher PCEs. In addition, we found that there was no significant difference in PCEs of the solar cells fabricated with HTM molecules bearing either –OMe groups (**6** & **10**) or the longer $-OC_6H_{13}$ chains (**7** & **11**), all of which demonstrated excellent PCEs of 15.28–17.10%. PSCs with **8** & **12** (–SMe groups), as expected, displayed relatively poor PCEs

Table 3 Photovoltaic performance of perovskite solar cells using **6–13** as hole-transporting layers.[ab]

HTMs		V_{oc} [V]	J_{sc} [mA cm^{-2}]	FF [%]	PCEs [%]
6	Best	1.05	21.41	75.50	16.96
	Average	1.02 ± 0.02	21.25 ± 0.42	73.40 ± 2.50	15.96 ± 0.92
7	Best	1.04	19.85	74.30	15.28
	Average	0.98 ± 0.04	19.73 ± 1.34	70.40 ± 5.50	13.61 ± 1.21
8	Best	0.87	19.99	22.80	3.95
	Average	0.60 ± 0.22	16.86 ± 3.36	30.90 ± 7.30	2.98 ± 0.93
9	Best	1.02	22.18	77.40	17.51
	Average	1.03 ± 0.01	22.00 ± 0.25	74.30 ± 2.20	16.82 ± 0.56
10	Best	1.06	21.37	73.30	16.61
	Average	1.02 ± 0.03	19.84 ± 1.39	74.30 ± 2.50	15.04 ± 1.04
11	Best	1.03	22.57	73.60	17.10
	Average	1.01 ± 0.01	22.07 ± 0.40	70.60 ± 6.80	15.82 ± 1.77
12	Best	0.87	14.68	61.00	7.78
	Average	0.81 ± 0.14	12.14 ± 1.63	66.00 ± 7.00	6.38 ± 1.24
13	Best	1.09	23.44	68.80	17.57
	Average	1.05 ± 0.02	22.20 ± 1.26	70.10 ± 1.00	16.42 ± 1.08
spiro-OMeTAD	Best	1.05	22.50	74.50	17.65
	Average	1.04 ± 0.01	21.59 ± 0.82	74.40 ± 1.60	16.77 ± 0.78

[a] Reverse scans. [b] Statistical data were calculated based on 6–8 cells.

(3.95%, 7.78%), which is consistent with the hole-mobility data acquired in Table 2.

Conclusions

Based on the optimized direct C–H arylation approach, we have efficiently synthesized eight new molecules bearing carbazole (**6–9**) or phenothiazine (**10–13**) cores in moderate to good isolated yields. Compared to traditional multistep synthesis, this step-saving synthetic methodology omitted previously required prefunctionalization steps such as deprotonative lithiation and transmetalation/stannylation. Perovskite solar cells fabrication using **6–13** as hole-transporting materials demonstrated power conversion efficiencies of 3.95–17.57%. Most noteworthy was that *t*-butyl substituted HTMs (**9** and **13**) exhibited exceptional hole-mobilities, thermal properties (high T_d and T_g), and the devices based on **9** or **13** displayed very promising power conversion efficiencies of 17.51–17.57%. Development of succinct synthetic routes combining direct C–H activation/arylation reactions[30] for the facile preparation of new small-molecule HTMs is currently underway in our laboratory.

Experimental

General procedure for the synthesis of 6–13

To a solution of $Pd(OAc)_2$ (15 mol%), P(*o*-tolyl)$_3$ (30 mol%), PivOH (60 mol%) and K_2CO_3 (3.60 equiv.) in DMF (3 mL) in a flame-dried Schlenk flask were added 3,6-dibromo-9-(4-bromophenyl)-9*H*-carbazole (**1**) or 3,7-dibromo-10-(4-bromophenyl)-10*H*-phenothiazine (**2**) (0.30 mmol) and the corresponding end-groups (**3a–d**) (0.96 mmol) under N_2. The reaction mixture was then heated at 125 °C under N_2 for 30 h. After the reaction mixture had cooled to room temperature, water (10 mL) was added. The mixture was extracted with dichloromethane (2 × 20 mL), and the combined organic layers were washed with brine (50 mL), dried (Na_2SO_4) and concentrated *in vacuo*. Purification by flash chromatography afforded the desired products **6–13**.

Conflicts of interest

There are no conflicts to declare.

Acknowledgements

Financial support provided by the Ministry of Science and Technology (MOST), Taiwan (MOST 108-2113-M-008-013 and 108-2628-E-182-003-MY3), National Central University (NCU), Chang Gung University (QZRPD181) and Chang Gung Memorial Hospital, Linkou, Taiwan (CMRPD2G0302 and CMRPD2J0041) are gratefully acknowledged. We also thank the instrument center (R & D office, NCU) for the technical support of NMR and mass analysis.

Notes and references

1 H. D. Pham, T. C.-J. Yang, S. M. Jain, G. J. Wilson and P. Sonar, Development of dopant-free organic hole transporting materials for perovskite solar cells, *Adv. Energy Mater.*, 2020, 1903326.
2 C. Rodriguez-Seco, L. Cabau, A. Vidal-Ferran and E. Palomares, Advances in the synthesis of small molecules as hole transport materials for lead halide perovskite solar cells, *Acc. Chem. Res.*, 2018, **51**, 869–880.
3 S. Ameen, M. A. Rub, S. A. Kosa, K. A. Alamry, M. S. Akhtar, H.-S. Shin, H.-K. Seo, A. M. Asiri and M. K. Nazeeruddin, Perovskite solar cells: influence of hole transporting materials on power conversion efficiency, *ChemSusChem*, 2016, **9**, 10–27.
4 L. Calió, S. Kazim, M. Grätzel and S. Ahmad, Hole-transport materials for perovskite solar cells, *Angew. Chem., Int. Ed.*, 2016, **55**, 14522–14545.
5 M. L. Petrus, K. Schutt, M. T. Sirtl, E. M. Hutter, A. C. Closs, J. M. Ball, J. C. Bijleveld, A. Petrozza, T. Bein, T. J. Dingemans, T. J. Savenije, H. Snaith and P. Docampo, New generation hole transporting materials for perovskite solar cells: amide-based small-molecules with nonconjugated backbones, *Adv. Energy Mater.*, 2018, 1801605.
6 D. E. M. Rojas, K. T. Cho, Y. Zhang, M. Urbani, N. Tabet, G. la Torre, M. K. Nazeeruddin and T. Torres, Tetrathienoanthracene and tetrathienylbenzene derivatives as hole-transporting materials for perovskite solar cell, *Adv. Energy Mater.*, 2018, 1800681.
7 C. Steck, M. Franckevicius, S. M. Zakeeruddin, A. Mishra, P. Bäuerle and M. Grätzel, A–D–A-type *S*,*N*-heteropentacene-based hole transport materials for dopant-free perovskite solar cells, *J. Mater. Chem. A*, 2015, **3**, 17738–17746.
8 A. Abate, S. Paek, F. Giordano, J. P. C. Baena, M. Saliba, P. Gao, T. Matsui, J. Ko, S. M. Zakeeruddin, K. H. Dahmen, A. Hagfeldt, M. Grätzel and M. K. Nazeeruddin, Silolothiophene-linked triphenylamines as stable hole transporting materials for high efficiency perovskite solar cells, *Energy Environ. Sci.*, 2015, **8**, 2946–2953.
9 C. Huang, W. Fu, C.-Z. Li, Z. Zhang, W. Qiu, M. Shi, P. Heremans, A. K.-Y. Jen and H. Chen, Dopant-free hole-transporting material with a C_{3h} symmetrical truxene core for highly efficient perovskite solar cells, *J. Am. Chem. Soc.*, 2016, **138**, 2528–2531.
10 Y. Liu, Z. Hong, Q. Chen, H. Chen, W.-H. Chang, M. Yang, T.-B. Song and Y. Yang, Perovskite solar cells employing dopant-free organic hole transport materials with tunable energy levels, *Adv. Mater.*, 2016, **28**, 440–446.
11 Y.-C. Chang, K.-M. Lee, C.-H. Lai and C.-Y. Liu, Direct C–H arylation meets perovskite solar cells: tin-free synthesis shortcut to high-performance hole-transporting materials, *Chem.–Asian J.*, 2018, **13**, 1510–1515; P.-H. Lin, K.-M. Lee, C.-C. Ting and C.-Y. Liu, Spiro-*t*BuBED: a new derivative of a spirobifluorene-based hole-transporting material for

efficient perovskite solar cells, *J. Mater. Chem. A*, 2019, **7**, 5934–5937; Y.-K. Peng, K.-M. Lee, C.-C. Ting, M.-W. Hsu and C.-Y. Liu, Making benzotrithiophene derivatives dopant-free for perovskite solar cells: step-saving installation of π-spacers by a direct C–H arylation strategy, *J. Mater. Chem. A*, 2019, **7**, 24765–24770.

12 A. Abudulimu, R. S. Torrientes, I. Zimmermann, J. Santos, M. K. Nazeeruddin and N. Martín, Hole transporting materials for perovskite solar cells and a simple approach for determining the performance limiting factors, *J. Mater. Chem. A*, 2020, **8**, 1386–1393.

13 K. Rakstys, S. Paek, A. Drevilkauskaite, H. Kanda, S. Daskeviciute, N. Shibayama, M. Daskeviciene, A. Gruodis, E. Kamarauskas, V. Jankauskas, V. Getautis and M. K. Nazeeruddin, Carbazole-terminated isomeric hole-transporting materials for perovskite solar cells, *ACS Appl. Mater. Interfaces*, 2020, **12**, 19710–19717.

14 C. H. Teh, R. Daik, E. L. Lim, C. C. Yap, M. A. Ibrahim, N. A. Ludin, K. Sopian and M. A. M. Teridi, A review of organic small molecule-based hole transporting materials for meso-structured organic–inorganic perovskite solar cells, *J. Mater. Chem. A*, 2016, **4**, 15788–15822.

15 S. F. Völker, S. Collavini and J. L. Delgado, Organic charge carriers for perovskite solar cells, *ChemSusChem*, 2015, **8**, 3012–3028.

16 J. Wang, K. Liu, L. Ma and X. Zhan, Triarylamine: versatile platform for organic, dye-sensitized, and perovskite solar cells, *Chem. Rev.*, 2016, **116**, 14675–14725.

17 W. Zhou, Z. Wen and P. Gao, Less is more: dopant-free hole transporting materials for high-efficiency perovskite solar cells, *Adv. Energy Mater.*, 2018, 1702512.

18 J. U. Mora, I. G. Benito, A. M. Ontoria and N. Martín, Hole transporting materials for perovskite solar cells: a chemical approach, *Chem. Soc. Rev.*, 2018, **47**, 8541–8571.

19 Z. Yu and L. Sun, Recent progress on hole-transporting materials for emerging organometal halide perovskite solar cells, *Adv. Energy Mater.*, 2015, **5**, 1500213.

20 S. J. Park, S. Jeon, I. K. Lee, J. Zhang, H. Jeong, J.-Y. Park, J. Bang, T. K. Ahn, H.-W. Shin, B.-G. Kim and H. J. Park, Inverted planar perovskite solar cells with dopant free hole transporting material: Lewis base-assisted passivation and reduced charge recombination, *J. Mater. Chem. A*, 2017, **5**, 13220–13227.

21 D. R. Kil, C. Lu, J.-M. Ji, C. H. Kim and H. K. Kim, Dopant-free triazatruxene-based hole transporting materials with three different end-capped acceptor units for perovskite solar cells, *Nanomaterials*, 2020, **10**, 936.

22 U. Bach, D. Lupo, P. Comte, J. E. Moser, F. Weissortel, J. Salbeck, H. Spreitzer and M. Grätzel, Solid-state dye-sensitized mesoporous TiO_2 solar cells with high photon-to-electron conversion efficiencies, *Nature*, 1998, **395**, 583–585; U. Bach, Y. Tachibana, J. E. Moser, S. A. Haque, J. R. Durrant, M. Grätzel and D. R. Klug, Charge separation in solid-state dye-sensitized heterojunction solar cells, *J. Am. Chem. Soc.*, 1999, **121**, 7445–7446; M. Liu, M. B. Johnston and H. J. Snaith, Efficient planar heterojunction perovskite solar cells by vapour deposition, *Nature*, 2013, **501**, 395–398; H. Zhou, Q. Chen, G. Li, S. Luo, T. B. Song, H. S. Duan, Z. Hong, J. You, Y. Liu and Y. Yang, Interface engineering of highly efficient perovskite solar cells, *Science*, 2014, **345**, 542–546.

23 Y. Wu, Z. Wang, M. Liang, H. Cheng, M. Li, L. Liu, B. Wang, J. Wu, R. P. Ghimire, X. Wang, Z. Sun, S. Xue and Q. Qiao, Influence of nonfused cores on the photovoltaic performance of linear triphenylamine-based hole-transporting materials for perovskite solar cells, *ACS Appl. Mater. Interfaces*, 2018, **10**, 17883–17895; Z. Li, Z. Zhu, C.-C. Chueh, S. B. Jo, J. Luo, S.-H. Jang and A. K.-Y. Jen, Rational design of dipolar chromophore as an efficient dopant-free hole-transporting material for perovskite solar cells, *J. Am. Chem. Soc.*, 2016, **138**, 11833–11839; B. Pashaei, S. Bellani, H. Shahroosvand and F. Bonaccorso, Molecularly engineered hole-transport material for low-cost perovskite solar cells, *Chem. Sci.*, 2020, **11**, 2429–2439.

24 K. Rakstys, A. Abate, M. I. Dar, P. Gao, V. Jankauskas, G. Jacopin, E. Kamarauskas, S. Kazim, S. Ahmad, M. Grätzel and M. K. Nazeeruddin, Triazatruxene-based hole transporting materials for highly efficient perovskite solar cells, *J. Am. Chem. Soc.*, 2015, **137**, 16172–16178; H. Choi, J. W. Cho, M. S. Kang and J. Ko, Stable and efficient hole transporting materials with a dimethylfluorenylamino moiety for perovskite solar cells, *Chem. Commun.*, 2015, **51**, 9305–9308; H. Choi, S. Park, S. Paek, P. Ekanayake, M. K. Nazeeruddin and J. Ko, Efficient star-shaped hole transporting materials with diphenylethenyl side arms for an efficient perovskite solar cell, *J. Mater. Chem. A*, 2014, **2**, 19136–19140; H. Choi, S. Paek, N. Lim, Y. H. Lee, M. K. Nazeeruddin and J. Ko, Efficient perovskite solar cells with 13.63% efficiency based on planar triphenylamine hole conductors, *Chem.–Eur. J.*, 2014, **20**, 10894–10899; K. Do, H. Choi, K. Lim, H. Jo, J. W. Cho, M. K. Nazeeruddin and J. Ko, Star-shaped hole transporting materials with a triazine unit for efficient perovskite solar cells, *Chem. Commun.*, 2014, **50**, 10971–10974; B. Xu, E. Sheibani, P. Liu, J. Zhang, H. Tian, N. Vlachopoulos, G. Boschloo, L. Kloo, A. Hagfeldt and L. Sun, Carbazole-based hole-transport materials for efficient solid-state dye-sensitized solar cells and perovskite solar cells, *Adv. Mater.*, 2014, **26**, 6629–6634; M. S. Kang, S. D. Sung, I. T. Choi, H. Kim, M. P. Hong, J. Kim, W. I. Lee and H. K. Kim, Novel carbazole-based hole-transporting materials with star-shaped chemical structures for perovskite-sensitized solar cells, *ACS Appl. Mater. Interfaces*, 2015, **7**, 22213–22217; C. Lu, I. T. Choi, J. Kim and H. K. Kim, Simple synthesis and molecular engineering of low-cost and star-shaped carbazole-based hole transporting materials for highly efficient perovskite solar cells, *J. Mater. Chem. A*, 2017, **5**, 20263–20276; S. Thokala and S. P. Singh, Phenothiazine-based hole transport materials for perovskite solar cells, *ACS Omega*, 2020, **5**, 5608–5619; J. Salunke, X. Guo, Z. Lin, J. R. Vale, N. R. Candeias, M. Nyman, S. Dahlström, R. Österbacka, A. Priimagi, J. Chang and P. Vivo, Phenothiazine-based hole-transporting materials toward ecofriendly perovskite

solar cells, *ACS Appl. Energy Mater.*, 2019, **2**, 3021–3027; J. Salunke, X. Guo, M. Liu, Z. Lin, N. R. Candeias, A. Priimagi, J. Chang and P. Vivo, N-substituted phenothiazines as environmentally friendly hole transporting materials for low-cost and highly stable halide perovskite solar cells, *ACS Omega*, 2020, **5**, 23334–23342; M. R. Maciejczyk, R. Chen, A. Brown, N. Zheng and N. Robertson, Beyond efficiency: phenothiazine, a new commercially viable substituent for hole transport materials in perovskite solar cells, *J. Mater. Chem. C*, 2019, **7**, 8593–8598; X. Liu, X. Tan, Q. Chen, H. Shan, C. Liu, J. Xu, Z.-K. Chen, W. Huang and Z.-X. Xu, Facile synthesis of a dopant-free hole transporting material with a phenothiazine core for planar perovskite solar cells, *RSC Adv.*, 2017, **7**, 53604–53610.

25 K.-M. Lu, K.-M. Lee, C.-H. Lai, C.-C. Ting and C.-Y. Liu, One-pot synthesis of D–π–D–π–D type hole-transporting materials for perovskite solar cells by sequential C–H (hetero)arylations, *Chem. Commun.*, 2018, **54**, 11495–11498.

26 M. Li, Z. Wang, M. Liang, L. Liu, X. Wang, Z. Sun and S. Xue, Low-cost carbazole-based hole-transporting materials for perovskite solar cells: influence of *S*,*N*-heterocycle, *J. Phys. Chem. C*, 2018, **122**, 24014–24024; J. Zhang, B. Xu, M. B. Johansson, N. Vlachopoulos, G. Boschloo, L. Sun, E. M. J. Johansson and A. Hagfeldt, Strategy to boost the efficiency of mixed-ion perovskite solar cells: changing geometry of the hole transporting material, *ACS Nano*, 2016, **10**, 6816–6825; J. Wu, C. Liu, B. Li, F. Gu, L. Zhang, M. Hu, X. Deng, Y. Qiao, Y. Mao, W. Tan, Y. Tian and B. Xu, Side-chain polymers as dopant-free hole-transporting materials for perovskite solar cells—the impact of substituents' positions in carbazole on device performance, *ACS Appl. Mater. Interfaces*, 2019, **11**, 26928–26937; H. Wang, A. D. Sheikh, Q. Feng, F. Li, Y. Chen, W. Yu, E. Alarousu, C. Ma, M. A. Haque, D. Shi, Z.-S. Wang, O. F. Mohammed, O. M. Bakr and T. Wu, Facile synthesis and high performance of a new carbazole-based hole-transporting material for hybrid perovskite solar cells, *ACS Photonics*, 2015, **2**, 849–855; J. A. Christians, P. Schulz, J. S. Tinkham, T. H. Schloemer, S. P. Harvey, B. J. T. Villers, A. Sellinger, J. J. Berry and and J. M. Luther, Tailored interfaces of unencapsulated perovskite solar cells for >1000 hour operational stability, *Nat. Energy*, 2018, **3**, 68–74; L. Gao, T. H. Schloemer, F. Zhang, X. Chen, C. Xiao, K. Zhu and A. Sellinger, Carbazole-based hole-transport materials for high-efficiency and stable perovskite solar cells, *ACS Appl. Energy Mater.*, 2020, **3**, 4492–4498; T. H. Schloemer, T. S. Gehan, J. A. Christians, D. G. Mitchell, A. Dixon, Z. Li, K. Zhu, J. J. Berry, J. M. Luther and A. Sellinger, Thermally stable perovskite solar cells by systematic molecular design of the hole-transport layer, *ACS Energy Lett.*, 2019, **4**, 473–482.

27 K. He, W. Li, H. Tian, J. Zhang, D. Yan, Y. Geng and F. Wang, Asymmetric conjugated molecules based on [1]benzothieno[3,2-*b*][1]benzothiophene for high-mobility organic thin-film transistors: influence of alkyl chain length, *ACS Appl. Mater. Interfaces*, 2017, **9**, 35427–35436; S. Inoue, H. Minemawari, J. Tsutsumi, M. Chikamatsu, T. Yamada, S. Horiuchi, M. Tanaka, R. Kumai, M. Yoneya and T. Hasegawa, Effects of substituted alkyl chain length on solution-processable layered organic semiconductor crystals, *Chem. Mater.*, 2015, **27**, 3809–3812.

28 I. Zimmermann, J. U. Mora, P. Gratia, J. Aragó, G. Grancini, A. M. Ontoria, E. Orti, N. Martin and M. K. Nazeeruddin, High-efficiency perovskite solar cells using molecularly engineered, thiophene-rich, hole-transporting materials: influence of alkyl chain length on power conversion efficiency, *Adv. Energy Mater.*, 2016, 1601674.

29 Q. Wang, E. Mosconi, C. Wolff, J. Li, D. Neher, F. Angelis, G. P. Suranna, R. Grisorio and A. Abate, Rationalizing the molecular design of hole-selective contacts to improve charge extraction in perovskite solar cells, *Adv. Energy Mater.*, 2019, **9**, 1900990; S. Lee, J. Lee, H. Park, J. Choi, H. W. Baac, S. Park and H. J. Park, Defect-passivating organic/inorganic bicomponent hole-transport layer for high efficiency metal-halide perovskite device, *ACS Appl. Mater. Interfaces*, 2020, **12**, 40310–40317.

30 L. Ackermann, Metalla-electrocatalyzed C–H activation by earth-abundant 3d metals and beyond, *Acc. Chem. Res.*, 2020, **53**, 84–104; P. Gandeepan, T. Müller, D. Zell, G. Cera, S. Warratz and L. Ackermann, 3d Transition metals for C–H activation, *Chem. Rev.*, 2019, **119**, 2192–2452; L. Ackermann, R. Vicente and A. R. Kapdi, Transition-metal-catalyzed direct arylation of (hetero)arenes by C–H bond cleavage, *Angew. Chem., Int. Ed.*, 2009, **48**, 9792–9826; T. Yanagi, S. Otsuka, Y. Kasuga, K. Fujimoto, K. Murakami, K. Nogi, H. Yorimitsu and A. Osuka, Metal-free approach to biaryls from phenols and aryl sulfoxides by temporarily sulfur-tethered regioselective C–H/C–H coupling, *J. Am. Chem. Soc.*, 2016, **138**, 14582–14585; C. Lu, M. Paramasivam, K. Park, C. H. Kim and H. K. Kim, Phenothiazine functionalized multifunctional A–π–D–π–D–π–A-type hole-transporting materials *via* sequential C–H arylation approach for efficient and stable perovskite solar cells, *ACS Appl. Mater. Interfaces*, 2019, **11**, 14011–14022.